Optics Letters

Frequency-tunable microwave generation with parity–time symmetry period-one laser dynamics

Xiaoyue Yu, Fangzheng Zhang,* Boyang Wu, Huihui Dai, Xinyi Li, and Shilong Pan

Key Laboratory of Radar Imaging and Microwave Photonics, Ministry of Education, Nanjing University of Aeronautics and Astronautics, Nanjing 210016, China

*Corresponding author: zhangfangzheng@nuaa.edu.cn

Received 2 January 2023; revised 1 February 2023; accepted 1 February 2023; posted 6 February 2023; published 2 March 2023

A novel frequency-tunable microwave signal generation method is proposed by incorporating parity–time (PT) symmetry in period-one (P1) laser dynamics in an optically injected semiconductor laser. In this method, P1 oscillation enables a large frequency tuning range and PT symmetry leads to excellent side-mode suppression and low phase noise. In an experimental demonstration, the side-mode suppression ratio reaches 58.4 dB and the phase noise is −126.2 dBc/Hz at 10 kHz offset when generating a 6.98 GHz signal, which are improved by 44.5 dB and 13.5 dB, respectively, compared with the previously reported optoelectronic oscillator-based P1 oscillation. By simply adjusting the optical injection strength, the frequency of the microwave signal generated by PT symmetry P1 dynamics is tuned from 5.07 GHz to 15.22 GHz, in which the phase noise is kept below 120 dBc/Hz at 10 kHz offset. The proposed method is expected to find applications in high-performance wireless communication and radar systems.

https://doi.org/10.1364/OL.484814

Low-phase-noise microwave signal sources having a large frequency-tunable range are highly desired in wireless communication and radar systems [1]. Conventional electric signal generators usually adopt frequency multiplication techniques to generate high-frequency microwave signals, which deteriorate the phase noise of generated signals. In recent years, photonic technologies have been applied to generate microwave signals with advantages including high frequency, large bandwidth, and resistance to electromagnetic interference [2–4]. Among the reported schemes, microwave signal generation using period-one (P1) dynamics in an optically injected semiconductor laser has attracted lots of attention, which features a compact structure and good flexibility [5,6]. By adjusting the injection parameters, the P1 oscillation frequency can be broadly tuned from a few gigahertz to over 100 GHz [7]. However, due to the intrinsic laser noise, the generated microwave signals usually have a large linewidth covering from several megahertz to 100 MHz. To deal with this problem, P1 oscillation with optical or optoelectronic feedbacks is proposed [8,9]. Among these schemes, the P1 oscillation incorporating an optoelectronic feedback loop comprises an optoelectronic oscillator (OEO), of which the spectral purity is obviously improved compared with typical P1 oscillation. However, the generated signal only achieves moderate level of phase noise and side-mode suppression ratio (SMSR), e.g., the phase noise of the signal generated in Ref. [9] is −114.04 dBc/Hz at 10 kHz offset. To meet the requirements of high-performance electric systems, the spectral purity still needs to be further improved.

In this Letter, we propose a new method to generate frequency-tunable low-phase-noise microwave signals by incorporating parity–time (PT) symmetry to P1 laser dynamics. In this system, P1 oscillation provides a large frequency tuning range and PT symmetry enables excellent mode selection by manipulating the gain and loss of two feedback loops. Through experimental investigations, the proposed PT symmetry P1 oscillation is proved to be capable of achieving much higher SMSR and lower phase noise compared with an OEO-based P1 oscillation system. When the loop length is ∼1 km, the generated microwave signals can be tuned from 5.07 to 15.22 GHz with a phase noise lower than −120 dBc/Hz at 10 kHz offset.

Figure 1 shows a schematic diagram of the proposed system. Continuous wave (CW) light from a master laser (ML) having a frequency of f_m is injected to a slave laser (SL) through an optical circulator (CIR). The SL is a semiconductor laser with a free-running frequency of f_s. Before the CIR, an optical attenuator (ATT) is used to adjust the optical injection power, and a polarization controller (PC1) is applied to align the polarization of the ML with that of the SL so as to maximize the injection efficiency. To excite P1 oscillation, the injection strength needs to be carefully adjusted at a given detuning frequency. Here, the injection strength ξ is defined as the square root of the optical injection power ratio divided by the output power of the free-running SL, and the detuning frequency f_i is the frequency difference between that of the ML and free-running SL ($f_i = f_m - f_s$) [6]. Since the optical injection consumes charge carriers and reduces the necessary gain in the SL, the cavity mode in the SL f_s' will be redshifted compared with the free-running frequency f_s through the anti-guidance effect [10]. The output signal from the SL mainly contains a regenerated carrier, a red-shifted optical sideband, and four-wave mixing (FMW) idlers. After the CIR, to improve the spectrum purity, an optical band-pass filter (OBPF) is used to remove the FMW idlers, and the output optical signal is passed through a span of single-mode fiber (SMF) with a high Q factor. To achieve PT symmetry, a polarization controller (PC2) combined with a polarization beam splitter (PBS) is used to split the optical signal into two

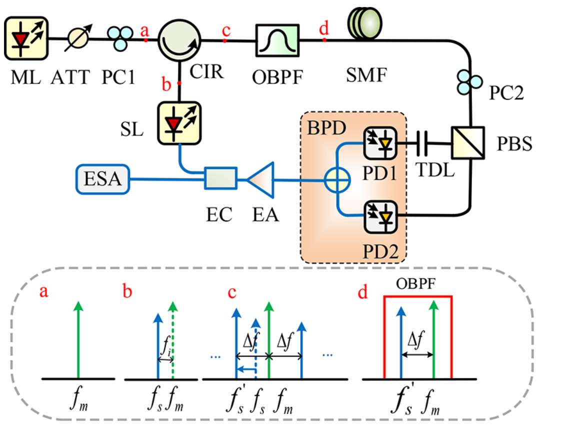

Fig. 1. Setup of the PT symmetry P1 oscillation system, where point b is the output of free-running SL without optical injection.

feedback loops, with one having a gain and the other having a loss. By adjusting PC2, the polarization direction of the incident light relative to the PBS can be altered to achieve a desired arbitrary power splitting ratio between the two loops. Then, the two optical signals are sent to a balanced photodetector (BPD) to perform optical-to-electrical conversion. In one of the feedback loops, a tunable optical delay line (TDL) is incorporated to offset the π phase shift introduced by the balance detection. Finally, the output of the BPD is amplified by an electrical amplifier (EA) and divided into two parts by an electrical coupler (EC). One part is fed back to the SL to form a closed feedback loop, and the other part is analyzed with an electrical spectrum analyzer (ESA).

Assuming the same delay in the two feedback loops, the longitudinal modes in the two loops have the same free spectral range (FSR). The PT symmetry is enabled by adjusting PC2 to ensure one loop has a net gain and the other loop has a net loss with the same magnitude. When the coupling coefficient between the two loops is smaller than the net gain and loss of the two loops, PT symmetry is broken and it is possible to allow a longitudinal mode with the highest gain to oscillate while the gains of other modes are below the oscillation threshold [11]. This way, single-mode oscillation is achieved. The gain difference between the highest mode g_0 and the next highest mode g_1 is

$$\Delta g_{\mathrm{PT}} = \sqrt{g_0^2 - g_1^2}, \quad (1)$$

while, for a traditional OEO, the gain difference between the highest and the next highest modes is

$$\Delta g = g_0 - g_1. \quad (2)$$

Because $g_0 > g_1$ is satisfied, the gain enhancement coefficient ($\Delta g_{\mathrm{PT}}/\Delta g$) of the PT symmetry method compared with the traditional OEO is greater than one. Thus, the PT symmetry method can enhance the gain difference and make the single-mode oscillation easier, which leads to higher SMSR and lower phase noise [12].

To verify the feasibility of the proposed method, an experiment is implemented based on the setup in Fig. 1. The ML is a narrow-linewidth laser (TeraXion) of which the wavelength can be tuned from 1528.77 to 1563.86 nm. The SL is a distributed-feedback semiconductor laser (Actech LD15DM) with a free-running wavelength of 1542.284 nm. It is biased

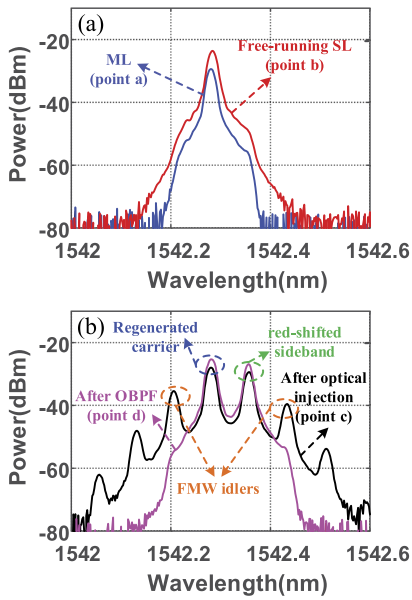

Fig. 2. Measured optical spectra of (a) free-running SL and ML and (b) signal after optical injection and signal after OBPF.

at 31.1 mA, about 5 times its threshold, and the free-running output power is 3.4 dBm. When the wavelength of the ML is tuned to 1542.28 nm, the optical spectra of the free-running SL and ML are measured using an optical spectrum analyzer (OSA, Yokogawa AQ6370D) with a resolution of 0.02 nm, as shown in Fig. 2(a). After optical injection, the regenerated optical carrier, redshifted sideband, and FMW idlers are generated, as shown in Fig. 2(b). After removing the FMW idlers using an OBPF (Yenista XTM-50), the spectrum of the obtained optical signal is shown in Fig. 2(b). The optical signal is launched to a span of SMF with a length of ∼1 km. The BPD (Finisar, BPDV2150R) has a bandwidth of 40 GHz. Two cascaded EAs (Mini-circuits) with a total gain of 40 dB and an operation bandwidth of 2–18 GHz are used to boost the RF power.

In the experiment, P1 oscillation property without feedback is first investigated by setting the optical injection parameters (f_i, ξ) to (0.5 GHz, 0.6). The generated microwave signal has a frequency of 6.98 GHz, and the spectrum is measured by an ESA (R&S RSWP-50) with a span of 100 MHz and a resolution bandwidth (RBW) of 100 kHz, as shown in Fig. 3. It is obvious that the generated signal has a large spectral width of several megahertz, because of the intrinsic noise of the semiconductor laser.

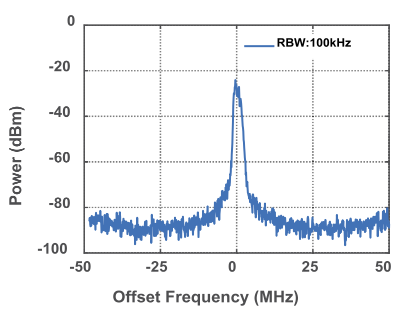

Fig. 3. Electrical spectrum of the microwave signal at 6.98 GHz generated without feedback.

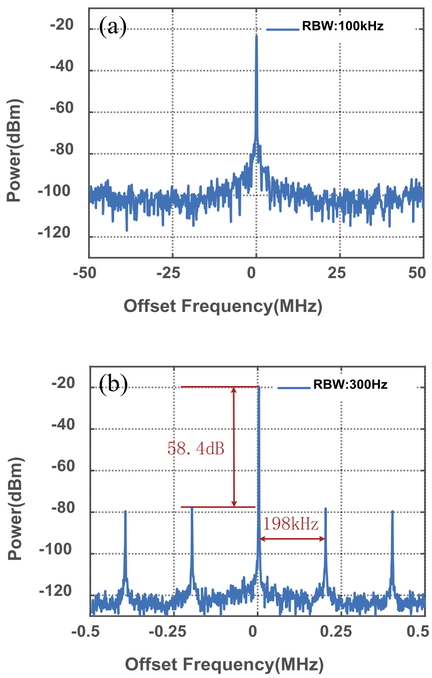

Fig. 4. Electrical spectra of the signal at 6.98 GHz generated by PT symmetry with (a) an observation span of 100 MHz and RBW of 100 kHz and (b) an observation span of 1 MHz and RBW of 300 Hz.

By closing the feedback loop and carefully adjusting PC2 to let the optical power injected to the two input ports of BPD be 2.8 dBm and −2.2 dBm, respectively, PT symmetry P1 oscillation state is achieved. Figure 4(a) shows the measured spectrum of the generated microwave signal with a span of 100 MHz and a RBW of 100 kHz. It is obvious that the generated signal spectrum is markedly narrowed compared with that in Fig. 3. Figure 4(b) shows the detailed electrical spectrum when the observation span is set to 1 MHz and the RBW is 300 Hz. It is observed that, although the side modes still exist, the SMSR reaches as high as about 58.4 dB. The side-mode spacing is found to be 198 kHz, which is consistent with the theoretical FSR determined by the loop length. As a comparison, the electrical spectrum of the signal generated using a traditional OEO structure is also measured, in which the optical signal transmitted through the same SMF is directly connected to a single-end PD for optical-to-electrical conversion and the electrical signal is fed to drive the SL to close the loop. The measured signal spectrum of the OEO-based P1 oscillation is shown in Fig. 5, in which the SMSR is about 13.9 dB. Therefore, the SMSR of the signal generated by PT symmetry P1 oscillation is improved by 44.5 dB compared with that of the signal generated by traditional OEO-based P1 oscillation.

The phase noises of signals generated by traditional OEO-based P1 oscillation and by PT symmetry P1 oscillation are measured as shown in Fig. 6, in which the phase noises at 10 kHz offset are −112.7 dBc/Hz and −126.2 dBc/Hz, respectively. According to this measurement, the phase noise at 10 kHz offset is improved by 13.5 dB by incorporating PT symmetry to P1 oscillation. It should also be mentioned that several peaks below 10 kHz offset appear in the phase noise curve of the OEO-based P1 oscillation, which is caused by the mode hopping effect. Clearly, these results can soundly confirm that the

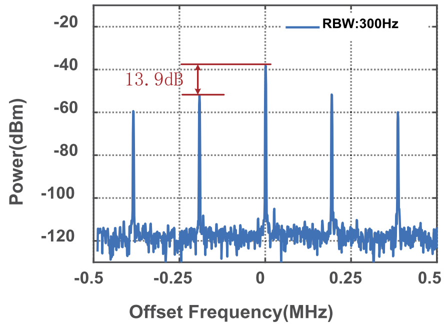

Fig. 5. Electrical spectrum of the signal at 6.98 GHz generated by traditional OEO with an observation span of 1 MHz and RBW of 300 Hz.

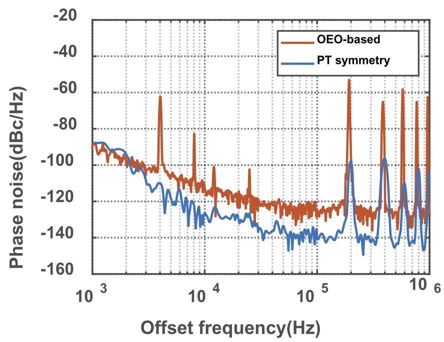

Fig. 6. Measured phase noise of generated 6.98 GHz signal by PT symmetry and traditional OEO with a loop length of ∼1 km.

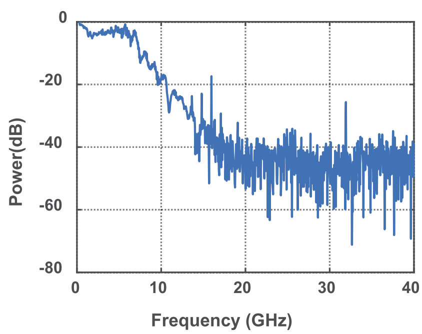

Fig. 7. Frequency response of the SL under direct modulation.

PT symmetry P1 oscillation can achieve much better phase noise performance and mode selection stability.

Finally, the frequency tuning property of the PT symmetry P1 oscillation system is investigated. Although P1 oscillation without feedback has a large frequency tuning range, the frequency tunability of our system is constrained, mainly due to the direct modulation bandwidth of the SL. Figure 7 shows the normalized frequency response of the SL, in which the 3 dB bandwidth is ∼7 GHz. In the experiment, the signal frequency is tuned by changing the optical injection power while fixing the detuning frequency. As long as the frequency responses of the feedback loops are stable and the electrical amplifiers can boost the signal power to a sufficiently high level, PT symmetry P1 oscillation can be achieved even if the oscillation frequency exceeds the 3 dB modulation bandwidth of the SL. Specifically, when tuning the optical injection power from −2.62 dBm

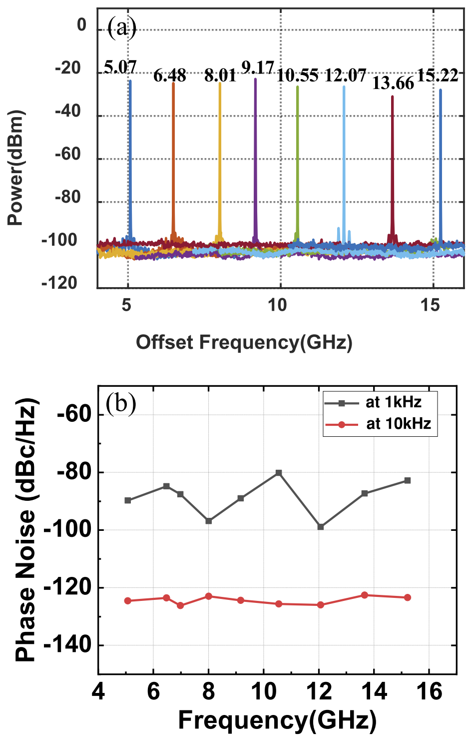

Fig. 8. (a) Measured spectral and (b) phase noise when generating microwave signals from 5.07 GHz to 15.22 GHz.

to 5.13 dBm (the corresponding injection strength varies from 0.50 to 1.22), the PT symmetry P1 oscillation system can generate microwave signals from 5.07 to 15.22 GHz. During the frequency tuning process, PC2 should be readjusted to control the net gain and loss between the two loops so as to meet the PT symmetry requirement. Figure 8(a) shows the spectra of several generated microwave signals and Fig. 8(b) shows the phase noise measurement results in which the phase noise is between −80.17 and −98.9 dBc/Hz at 1 kHz offset, and between −122.56 and −126.2 dBc/Hz at 10 kHz offset. If the optical injection power is further increased, although higher-frequency microwave signals can be generated, the phase noises will be deteriorated, e.g., the phase noise of generated signal at 17 GHz is −116.92 dBc/Hz at 10 kHz offset. This is caused by the fact that the loop gain cannot support high-Q oscillation at such high frequencies because of the reduced power responses of the SL. To cope with this problem and enlarge the frequency range for high-quality signal generation, a SL with larger modulation bandwidth and/or amplifiers providing more gain can be applied.

In conclusion, we have demonstrated a frequency-tunable microwave generation method by incorporating PT symmetry into P1 laser dynamics. When generating a 6.98 GHz signal, the SMSR and phase noise at 10 kHz offset are improved by 44.5 dB and 13.5 dB, respectively, compared with the traditional OEO-based method. Frequency tunability of this method is also demonstrated, in which microwave signals from 5.07 to 15.22 GHz with phase noise lower than −120 dBc/Hz at 10 kHz are generated.

Funding. National Key Research and Development Program of China (2021YFB2800803); Natural Science Foundation of Jiangsu Province (BK20221479); Open Project Program of Wuhan National Laboratory for Optoelectronics (2022WNLOKF002); Open Fund of State Key Laboratory of Advanced Optical Communication Systems and Networks (2023GZKF03); Fund of Prospective Layout of Scientific Research for NUAA.

Disclosures. The authors declare no conflicts of interest.

Data availability. Data underlying the results presented in this Letter are not publicly available at this time but may be obtained from the authors upon reasonable request.

REFERENCES

1. J. Yao, J. Lightwave Technol. **27**, 314 (2009).
2. F. Zhang, G. Sun, Y. Zhou, B. Gao, and S. Pan, IEEE J. Sel. Top. Quantum Electron. **28**, 1 (2022).
3. F. Zhang, Q. Guo, and S. Pan, Sci. Rep. **7**, 13848 (2017).
4. X. S. Yao and L. Maleki, IEEE J. Quantum Electron. **32**, 1141 (1996).
5. S. C. Chan, S. K. Hwang, and J. Liu, Opt. Express **15**, 14921 (2007).
6. X. Yu, G. Sun, F. Zhang, and S. Pan, Opt. Lett. **47**, 5921 (2022).
7. E. K. Lau, X. Zhao, H.-K. Sung, D. Parekh, C. Chang-Hasnain, and M. C. Wu, Opt. Express **16**, 6609 (2008).
8. J.-P. Zhuang and S.-C. Chan, Opt. Lett. **38**, 344 (2013).
9. P. Zhou, F. Zhang, D. Zhang, and S. Pan, Opt. Lett. **43**, 5439 (2018).
10. S. C. Chan, IEEE J. Quantum Electron. **46**, 421 (2010).
11. J. Zhang and J. Yao, Sci. Adv. **4**, eaar6782 (2018).
12. C. Teng, X. Zou, P. Li, W. Pan, and L. Yan, J. Lightwave Technol. **38**, 5406 (2020).